Quantum Electronics **41** (6) 571–576 (2011)

RESONATORS

PACS numbers: 42.60.Da; 42.25.Ja; 42.55.Sa
DOI: 10.1070/QE2011v041n06ABEH014562

Nonorthogonal polarisation eigenstates in anisotropic cavities

Yu.A. Mamaev, P.A. Khandokhin

Abstract. **The Jones matrix method is used to analyse the polarisation eigenmodes of a solid-state laser with an anisotropic Fabry–Perot cavity containing amplitude and phase anisotropic elements. The results demonstrate that, when the axes of these elements do not coincide, the eigenpolarisations become elliptical and nonorthogonal. The ellipticities and azimuths of the polarisation modes and the magnitude and phase of the nonorthogonality parameter are determined as functions of polariser angle at different relationships between the amplitude and phase anisotropies, and the effect is shown to be strongest at a polariser angle of 45°. There is critical phase anisotropy, dependent on amplitude anisotropy, at which the magnitude of the nonorthogonality parameter and ellipticity of the polarisation modes approach unity.**

Keywords: *phase anisotropy, amplitude anisotropy, polarisation mode, nonorthogonality parameter, pump-induced gain anisotropy, Fabry–Perot cavity, microchip lasers, Jones matrix method.*

1. Introduction

Modes generated in multimode lasers are usually assumed to be orthogonal, which is typically quite justified but is not always the case. Mode nonorthogonality means that there is linear coupling between the modes. The result is excess noise, which considerably broadens the laser emission line [1, 2]. In ring lasers, linear coupling between counterpropagating cavity modes may cause self-modulation oscillations [3–6]. In this paper, we consider several model problems that highlight some common properties of polarisation eigenstates in anisotropic cavities. These properties are rather important and should be taken into account in describing laser dynamics.

One effective way to assess laser radiation dynamics is to expand the electromagnetic field in the laser cavity in terms of its eigenmodes. Further, one can expand the population inversion in terms of the cavity eigenmodes and derive equations for each particular mode. In this approach, one usually selects a basis of orthogonal modes whose polarisations are specified at the outset and do not vary in space [7]. This approach is however not always rigorous: eigenmodes are orthogonal only in the case of an isotropic cavity, whereas the modes of a cavity that possesses phase or amplitude anisotropy may be nonorthogonal. It is therefore important to take into account the mutual orientation of the eigenaxes of anisotropic elements.

Cavity anisotropy is not always caused directly by anisotropic elements placed in the cavity. Sometimes, this is simply impossible, e.g. when the cavity is very short (chip laser) or mirrors are deposited directly onto crystal faces. There may be other causes of anisotropy, in particular, pump-induced anisotropy (for example, linearly polarised radiation from a semiconductor laser leads to gain anisotropy [8, 9]). An external magnetic field or internal-stress-induced residual birefringence produces phase anisotropy. This means that there is always at least a small anisotropy and it has to be taken into account under some conditions.

This paper examines the behaviour of eigenpolarisations of a system. In connection with this, it is worth while to specify the assumptions used below. The modes in a Fabry–Perot cavity have longitudinal and transverse structures and polarisations. Resonance conditions require the formation of standing waves along the length of the cavity, which eventually ensures orthogonality of different longitudinal modes. Of the transverse modes, there is usually only the fundamental one, which has the lowest loss (the other transverse modes can be eliminated by an aperture). Therefore, in what follows the transverse beam structure can be left out of consideration and each cavity mode can be thought of as a standing plane wave. The question of coupling between polarisation modes having the same longitudinal index remains open. This issue will be addressed in what follows. Mode coupling is rather difficult to assess, which typically requires numerical simulations. At the same time, because polarisation modes are considered, there are approximations that can significantly simplify the problem.

Neglecting diffraction, the variation of the cavity and beam parameters with the transverse coordinates (i.e., considering the system near the cavity axis), and frequency dispersion, one can calculate eigenpolarisations using the Jones matrix method. This method allows one to find the polarisation of eigenmodes at any point of the cavity and to calculate their quality factors and frequency difference. The results thus obtained provide answers to a number of questions regarding the key features of eigenpolarisations, dual- or single-polarisation operation of the laser and coupling between its eigenmodes.

The purpose of this work is to identify common features in the polarisation properties of anisotropic cavities using particular model problems as examples.

2. Linear cavity with a partial polariser and a wave plate

Consider an anisotropic cavity containing anisotropic elements with amplitude and phase anisotropies. The residual

Yu.A. Mamaev, P.A. Khandokhin Institute of Applied Physics, Russian Academy of Sciences, ul. Ul'yanova 46, 603950 Nizhnii Novgorod, Russia; e-mail: myua@appl.sci-nnov.ru, khando@appl.sci-nnov.ru

Received 14 February 2011
Kvantovaya Elektronika **41** (6) 571–576 (2011)
Translated by O.M. Tsarev

birefringence of an active element can be modelled by a wave plate of phase thickness θ. The x and y axes of the Cartesian coordinate system are parallel to the axes of the wave plate, as shown in Fig. 1. In addition, the cavity contains a partial polariser with a rotation angle φ relative to the x axis, which models the gain anisotropy induced by linearly polarised pump light [8–10]. Rotation of the plane of polarisation of the pump light through an angle φ means rotation of the polariser through the same angle. It is convenient to perform calculations for an anisotropic cavity using the Jones matrix method [11].

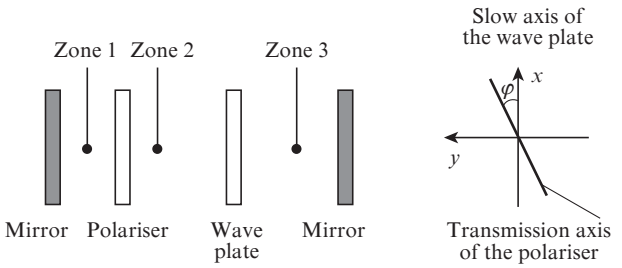

Figure 1. Schematic of a Fabry–Perot cavity with an intracavity polariser and wave plate making an angle φ.

In this method, the polarisation eigenstates of a cavity can be found by constructing a cavity round-trip Jones matrix $\boldsymbol{M}$ and determining the eigenvectors $\boldsymbol{u}$ and eigenvalues λ of the matrix:

$$\boldsymbol{M} = \boldsymbol{M}_n \boldsymbol{M}_{n-1} \ldots \boldsymbol{M}_2 \boldsymbol{M}_1, \qquad \boldsymbol{M}\boldsymbol{u} = \lambda \boldsymbol{u}. \tag{1}$$

We will consider eigenvectors in the form

$$\boldsymbol{u} = E_x \begin{pmatrix} 1 \\ \chi \end{pmatrix}, \tag{2}$$

where $\chi = E_y/E_x$ is a complex-valued polarisation parameter which can be used to determine ellipticity ε (the ratio of the minor axis to the major axis of the polarisation ellipse) and azimuth β (the angle between the semimajor axis of the polarisation ellipse and the x axis) [12, 13]:

$$\varepsilon = \tan\left[\frac{1}{2}\arcsin\left(\frac{2\,\mathrm{Im}\chi}{1+|\chi|^2}\right)\right], \qquad \beta = \frac{1}{2}\arctan\left(\frac{2\,\mathrm{Re}\chi}{1-|\chi|^2}\right) + \frac{n\pi}{2}. \tag{3}$$

Here $n = 0$ for one polarisation mode and $n = 1$ for the other.

Equation (1) has a solution in the form of two eigenvectors, $\boldsymbol{u}_{1,2}$, and accordingly two eigenvalues, $\lambda_{1,2}$. The eigenvalues can be expressed through the matrix elements $\boldsymbol{M}_{ij}$:

$$\lambda_{1,2} = \mathrm{Tr}(\boldsymbol{M})/2 \pm \sqrt{\mathrm{Tr}^2(\boldsymbol{M})/4 - \det(\boldsymbol{M})}, \tag{4}$$

where $\mathrm{Tr}(\boldsymbol{M}) = M_{11} + M_{22}$ and $\det(\boldsymbol{M}) = M_{11}M_{22} + M_{12}M_{21}$. The complex-valued polarisation parameters are given by

$$\chi_{1,2} = \frac{\lambda_{1,2} - M_{11}}{M_{12}} = \frac{M_{21}}{\lambda_{1,2} - M_{22}}. \tag{5}$$

To characterise the nonorthogonality of polarisation eigenmodes, we use the parameter

$$g = \frac{(\boldsymbol{u}_1 \boldsymbol{u}_2^*)}{|\boldsymbol{u}_1||\boldsymbol{u}_2|} = \frac{1 + \chi_1 \chi_2^*}{\sqrt{\left(1+|\chi_1|^2\right)\left(1+|\chi_2|^2\right)}} = |g|\exp(\mathrm{i}\arg g); \tag{6}$$

where $0 \leqslant |g| \leqslant 1$. The condition $g = 0$ means that there is no linear coupling between the polarisation modes.

Since we are interested in the state of polarisation modes in an active medium, we will consider polarisation parameters in zone 2 of an anisotropic cavity (Fig. 1). Matrix $\boldsymbol{M}$ in zone 2 can be represented in the form

$$\boldsymbol{M} = r_1 r_2 \boldsymbol{F}^2 \boldsymbol{R}(\varphi) \boldsymbol{P}^2 \boldsymbol{R}(-\varphi). \tag{7}$$

Here,

$$\boldsymbol{P} = \begin{pmatrix} 1 & 0 \\ 0 & 1-b \end{pmatrix}$$

is the matrix of the partial polariser (the parameter $b < 1$ specifies the amplitude anisotropy);

$$\boldsymbol{F} = \begin{pmatrix} \exp(\mathrm{i}\theta/2) & 0 \\ 0 & \exp(-\mathrm{i}\theta/2) \end{pmatrix}$$

is the matrix of the wave plate;

$$\boldsymbol{R}(\varphi) = \begin{pmatrix} \cos\varphi & -\sin\varphi \\ \sin\varphi & \cos\varphi \end{pmatrix}$$

is the matrix for rotation through an angle φ; and $r_{1,2}$ are the reflectivities of the mirrors.

Multiplying the matrices in (7) and introducing $\tilde{b} = b(1 - b/2)$, we obtain

$$\boldsymbol{M}/r_1 r_2 = \begin{pmatrix} \exp(\mathrm{i}\theta)(1 - 2\tilde{b}\sin^2\varphi) & \exp(\mathrm{i}\theta)\tilde{b}\sin 2\varphi \\ \exp(-\mathrm{i}\theta)\tilde{b}\sin 2\varphi & \exp(-\mathrm{i}\theta)(1 - 2\tilde{b}\cos^2\varphi) \end{pmatrix}. \tag{8}$$

The eigenvalues λ in (4) determine the loss in the cavity, $p = 1 - |\lambda|^2$, and the correction to the polarisation mode frequencies:

$$f = \Delta\nu/\nu_0 = \arg\lambda/(2\pi),$$

where $\nu_0 = c/(2L_{\mathrm{opt}})$ is the mode spacing (c is the speed of light and L_{opt} is the optical length of the cavity).

General expressions for the polarisation parameters ε and β and the nonorthogonality parameter g are difficult to derive. Illustrative expressions for these parameters can only be obtained in two limits: when the phase anisotropy is small compared to the amplitude anisotropy and in the opposite case.

Consider first the case of small phase anisotropy. For

$$\theta \ll \tilde{b}, \tag{9}$$

the radicand in (4) can be expanded in terms of a small parameter. Retaining only the first-order terms, we obtain after simple transformations

$$\varepsilon_1 \approx -\sin(2\theta)\sin(2\varphi)/(4\tilde{b}),$$

$$\varepsilon_2 \approx -(1-2\tilde{b})\sin(2\theta)\sin(2\varphi)/(4\tilde{b}),$$

$$\beta_1 \approx \varphi, \qquad (10)$$

$$\beta_2 \approx \pi/2 + \varphi,$$

$$g \approx \mathrm{i}(1-\tilde{b})\sin(2\theta)\sin(2\varphi)/(2\tilde{b}).$$

It can be seen from (10) that the ellipticities of the two polarisation modes, $\varepsilon_{1,2}$, differ in magnitude and have the same sign. They reach their maximum values at $\varphi = \pi/4$ and $3\pi/4$, as does the magnitude of the nonorthogonality parameter g. The ellipticities $\varepsilon_{1,2}$ and the magnitude of g increase with decreasing b [when condition (9) is fulfilled].

The azimuth of the polarisation ellipse specifies the rotation angle of the anisotropic-amplitude element. To first order in $\theta/\tilde{b}$, the azimuth difference is $\pi/2$.

In the case of small amplitude anisotropy, the radicand in (4) can be expanded into a power series when the following conditions are fulfilled:

$$\tilde{b} \ll 1, \quad \tilde{b} \ll \tan\theta. \qquad (11)$$

Omitting intermediate steps, we give the final expressions for the ellipticities $\varepsilon_{1,2}$, azimuths $\beta_{1,2}$ and nonorthogonality parameter g:

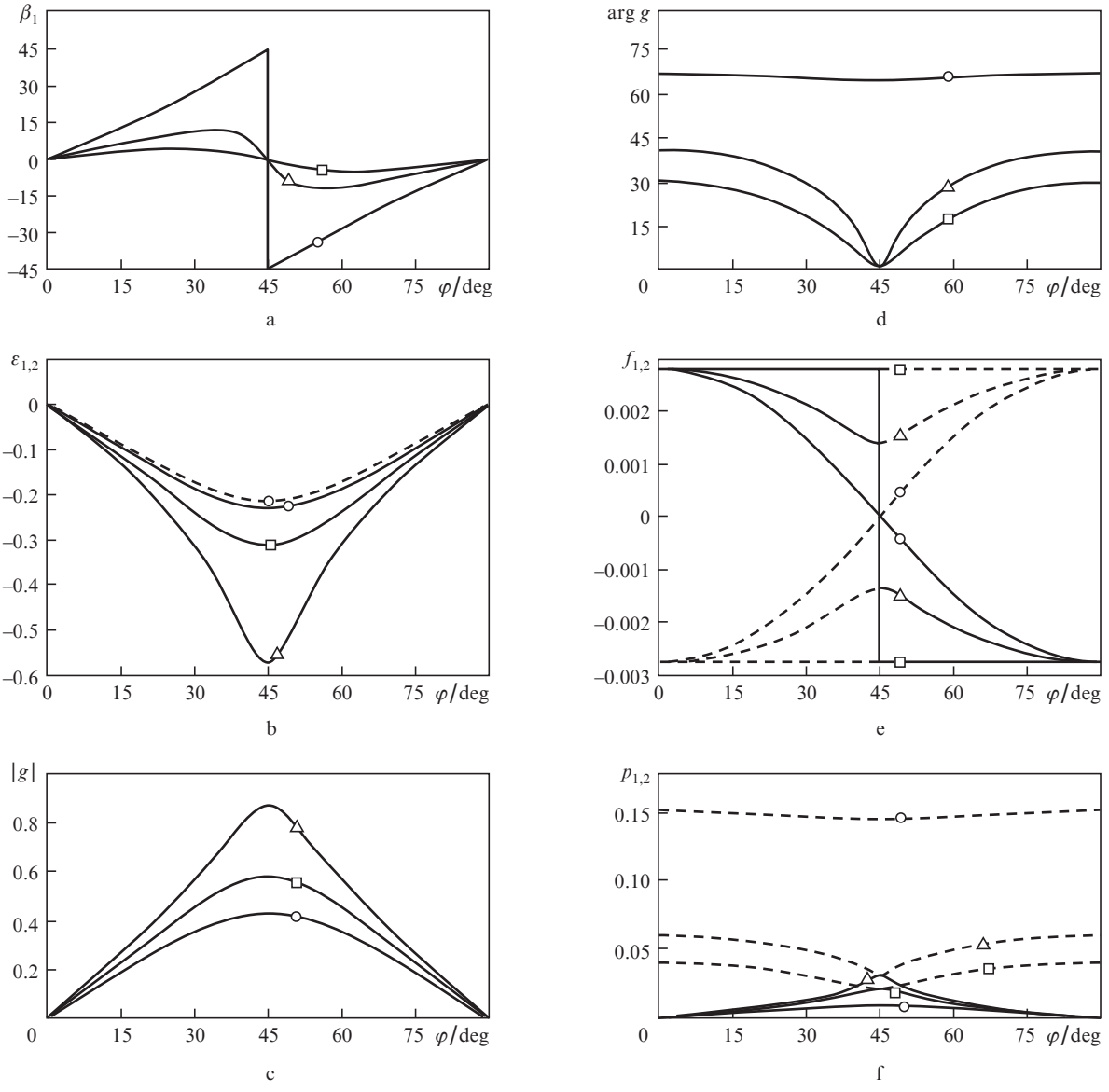

Figure 2. Azimuth β_1, ellipticities $\varepsilon_{1,2}$, magnitude and phase of the nonorthogonality parameter g, frequency corrections $f_{1,2}$ and losses $p_{1,2}$ as functions of polariser angle, φ, for the two polarisation modes at an amplitude anisotropy $b = 0.01$ (□), 0.015 (△) and 0.04 (○) and a phase anisotropy $\theta = 1°$ (0.0175 rad). Here and in what follows, the data for the subscript 1 are represented by solid lines and those for the subscript 2 are represented by dashed lines.

$$\varepsilon_1 = \varepsilon_2 \approx -\tan\left[0.5\arcsin\left(\frac{2Ab\sin(2\theta)\tan\varphi}{4 + A^2b^2\sin^2\theta\tan^2\varphi}\right)\right],$$

$$\beta_1 \approx -\frac{1}{2}\arctan\left(\frac{4Ab\sin^2\theta\tan\varphi}{4 - A^2b^2\sin^2\theta\tan^2\varphi}\right), \qquad (12)$$

$$\beta_2 \approx \pi/2 + \beta_1,$$

$$g \approx -\frac{4Ab\sin\theta\tan\varphi}{4 - A^2b^2\sin^2\theta\tan^2\varphi},$$

where $A = 1 + 2\cot^2\theta\cos^2\varphi$. It follows from (12) that the ellipticities of the two polarisation modes are equal in magnitude and have the same sign. Accordingly, the azimuths of the polarisation ellipses are close to zero and $\pi/2$ because of the small amplitude anisotropy b. The azimuth difference generally differs from $\pi/2$ by the small quantity $2\beta_1$.

3. Numerical simulation results

The mode polarisation and nonorthogonality parameters of a Fabry–Perot cavity (Fig. 1) were evaluated numerically using the exact expressions (4)–(8). Figure 2 shows characteristics of cavity polarisation modes as functions of polariser angle, φ, at a phase thickness $\theta = 1°$ (0.0175 rad) and different amplitude anisotropy values, b. At a small amplitude anisotropy ($b = 0.01 < \theta$, Fig. 2a), the orientations of the polarisation modes are essentially independent of polariser orientation (large phase anisotropy), whereas for $b = 0.04 > \theta$ the azimuths of the polarisation modes specify the polariser orientation, φ. This corresponds to large amplitude anisotropy.

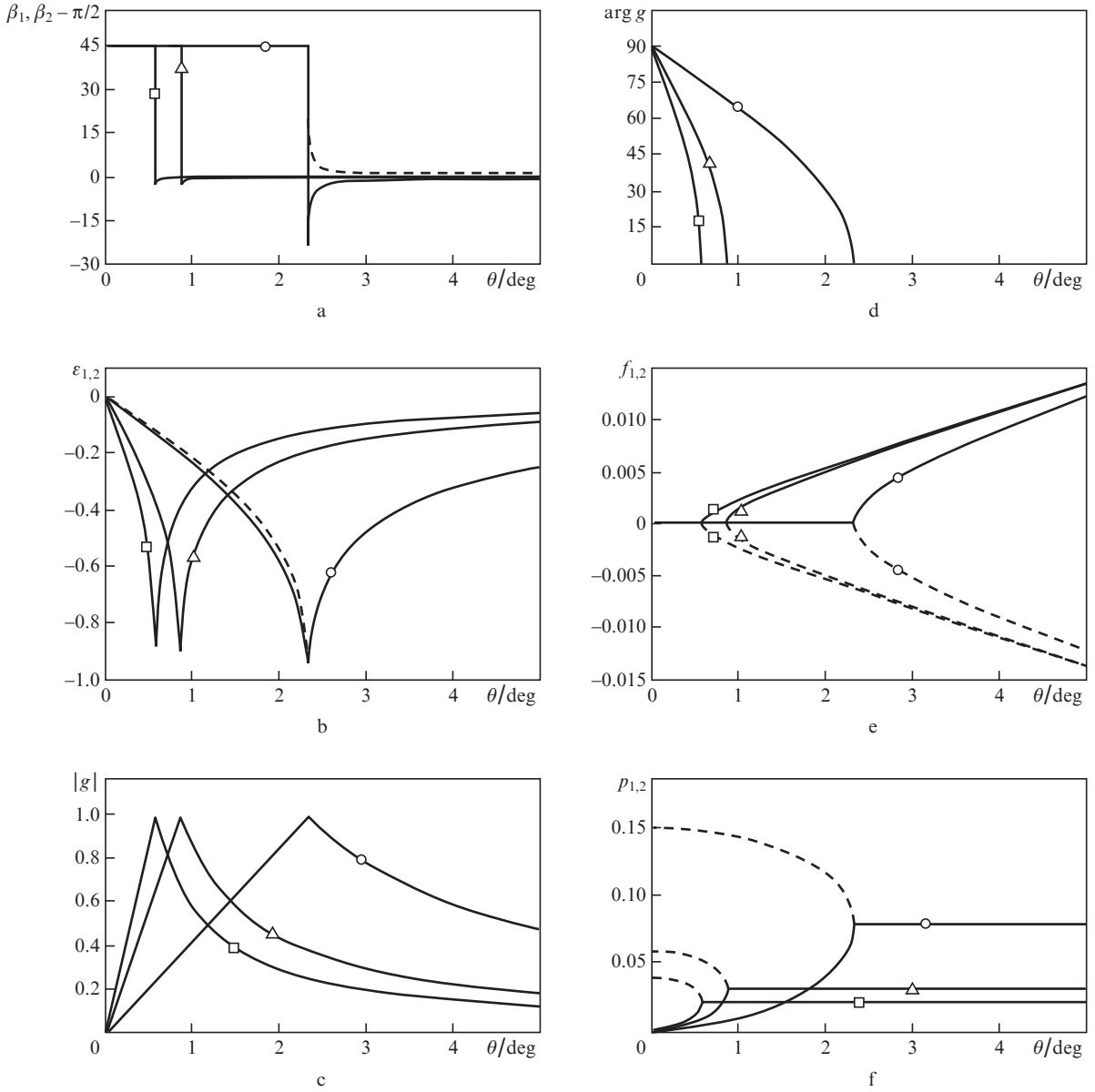

Figure 3. Azimuths β_1 and $\beta_2 - \pi/2$, ellipticities $\varepsilon_{1,2}$, magnitude and phase of the nonorthogonality parameter g, frequency corrections $f_{1,2}$ and losses $p_{1,2}$ as functions of phase anisotropy, θ, for the two polarisation modes at an amplitude anisotropy $b = 0.01$ (□), 0.015 (△) and 0.04 (○) and a polariser angle $\varphi = 45°$.

The variations in the azimuths of the eigenpolarisations with polariser angle are accompanied by variations in the ellipticities $\varepsilon_{1,2}$ (Fig. 2b) and the magnitude and phase of the nonorthogonality parameter (Figs 2c, 2d). As seen, $\varepsilon_{1,2}$ have the maximum magnitude at $\varphi = 45°$. The ellipticities then have the same sign and differ in magnitude (solid and dashed lines). The curves for the magnitude of the nonorthogonality parameter, $|g|$, have a similar shape (Fig. 2c). Figure 2d shows the $\arg g$ curves. At small θ, $\arg g$ varies little, with a minimum at $\varphi = 45°$. With increasing θ, the variations become more significant, and $\arg g$ drops to zero at $\varphi = 45°$. Figure 2e shows the corrections to the frequencies of the two polarisation modes (normalised to the mode spacing) as functions of φ. For $b \geqslant \theta$ (the amplitude anisotropy is comparable to the phase anisotropy), the initial frequency difference due to phase anisotropy varies considerably.

To assess the influence of the phase thickness of the wave plate, θ, on the polarisation characteristics and nonorthogo-

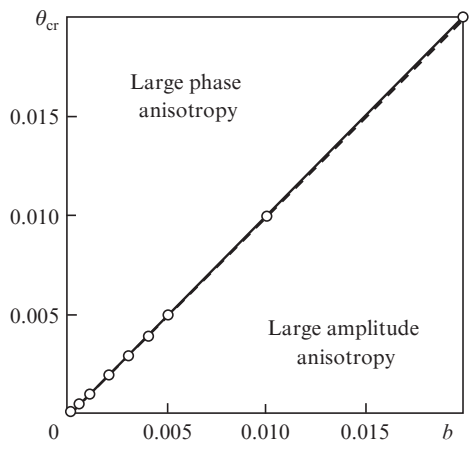

Figure 4. Critical phase anisotropy, θ_{cr}, against amplitude anisotropy, b, at a polariser angle $\varphi = 45°$.

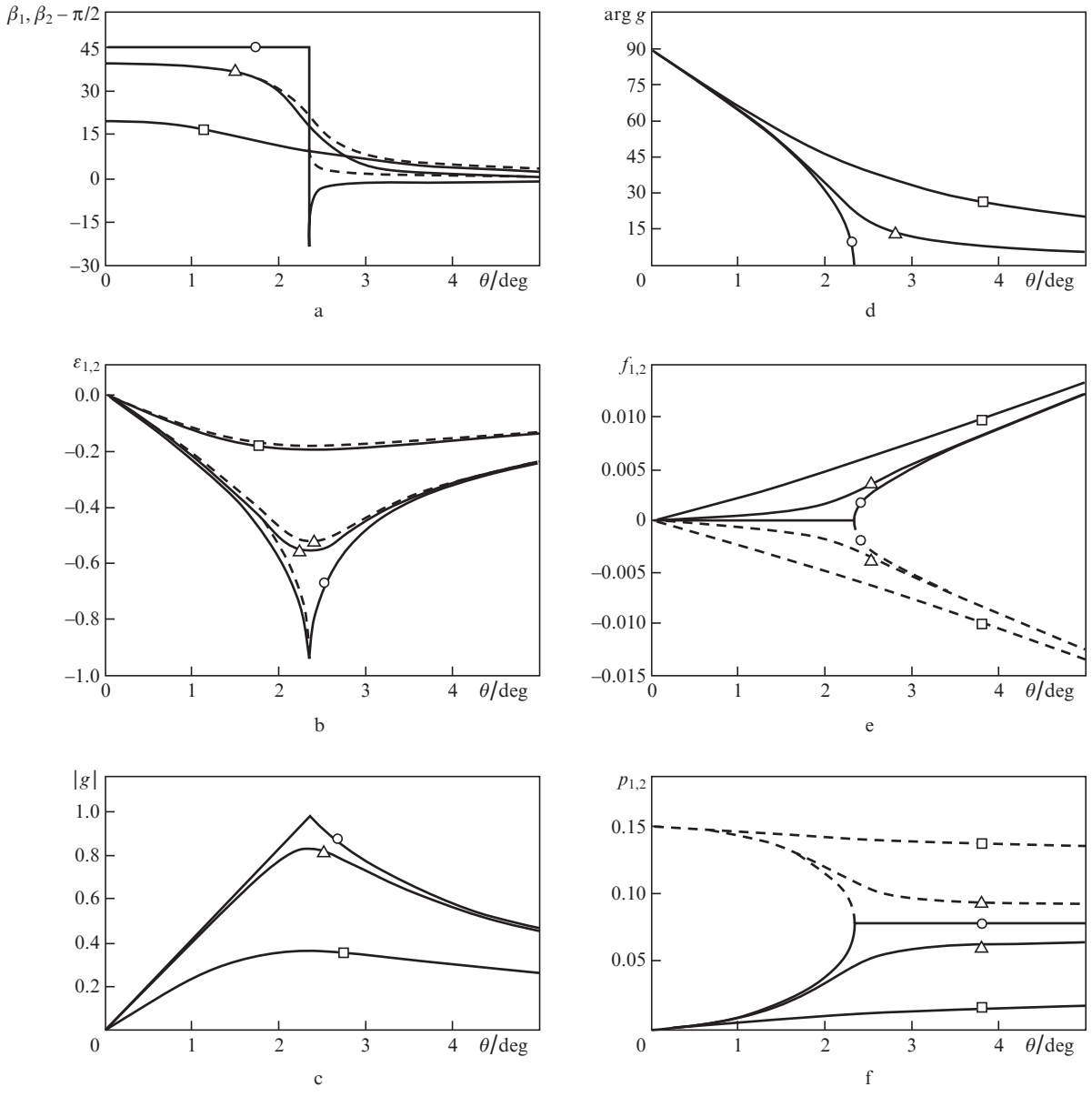

Figure 5. Azimuths β_1 and $\beta_2 - \pi/2$, ellipticities $\varepsilon_{1,2}$, magnitude and phase of the nonorthogonality parameter g, frequency corrections $f_{1,2}$ and losses $p_{1,2}$ as functions of phase anisotropy, θ, for the two polarisation modes at a polariser angle $\varphi = 45°$ (□), 40° (△) and 20° (○) and $b = 0.04$.

nality parameter, we calculated $\varepsilon_{1,2}, \beta_{1,2}$, $|g|$ and arg$g$ as functions of θ at a polariser angle $\varphi = 45°$ and different values of amplitude anisotropy, b. The results are presented in Fig. 3. It is seen that, at a certain low value $\theta = \theta_{cr}$, dependent on b, the eigenpolarisations may approach circular configurations, and the magnitude of the nonorthogonality parameter then approaches unity (Figs 3b, 3c). With increasing amplitude anisotropy, b, the value of θ_{cr}, corresponding to the maximum in $\varepsilon_{1,2}$, shifts to greater phase thicknesses.

At a wave plate thickness θ_{cr}, the azimuths drop by $\sim 45°$ at $\varphi = 45°$ (Fig. 3a). Figure 4 plots θ_{cr} against b (dashed line). The data are well represented by the linear relation $\theta_{cr} = b$ (solid line). The straight line separates the regions of large and small amplitude anisotropy.

Figure 5 shows the polarisation and nonorthogonality parameters as functions of phase thickness, θ, at different partial polariser angles (45°, 40° and 20°) and $b = 0.04$. At $\varphi = 45°$, the ellipticities of the two polarisation modes have the largest magnitude (nearly circular polarisations) and the orthogonality parameter approaches unity. At φ less or greater than 45°, the curves have a similar shape, but the above parameters are considerably smaller, especially at $\theta \approx \theta_{cr}$.

Analysis of the polarisation modes in zones 1 and 3 (Fig. 1) indicates that the above relations remain almost unchanged, but the ellipticities in these zones are the same for the two polarisation modes and are half the sum of the ellipticities in zone 2.

4. Conclusions

The present simulations demonstrate that linearly polarised pump light induces amplitude anisotropy that may have – in combination with the residual phase anisotropy of the active element – a significant effect on the polarisations of the two cavity eigenmodes, leading to their nonorthogonality (and accordingly to coupling and interaction between these modes in the active medium). The polarisation eigenmodes are orthogonal only when the eigenaxes of the polariser coincide with those of the anisotropic-phase medium. Linear amplitude anisotropy can be prevented by employing circularly polarised or unpolarised pump light.

Acknowledgements. This work was supported by the RF President's Grants Council (Support to Leading Scientific Schools Programme, Grant No. NSh-3800.2010.2).

References

1. Petermann K. *IEEE J. Quantum Electron.*, **QE-15**, 566 (1979).
2. Khanin Ya.I. *Izv. Vyssh. Uchebn. Zaved., Ser. Radiofiz.*, **47**, 799 (2004).
3. Khandokhin P.A., Khanin Ya.I. *J. Opt. Soc. Am. B*, **2**, 226 (1985).
4. Zolotoverkh I.I., Kravtsov N.V., Lariontsev E.G., Makarov A.A., Firsov V.V. *Opt. Commun.*, **113**, 249 (1994).
5. Kravtsov N.V., Lariontsev E.G. *Kvantovaya Elektron.*, **36**, 192 (2006) [*Quantum Electron.*, **36**, 192 (2006)].
6. Sorel M., Giuliani G., Scire A., Miglierina R., Donati S., Laybourn P.J.R. *IEEE J. Quantum Electron.*, **39**, 1187 (2003).
7. Khandokhin P.A. *Kvantovaya Elektron.*, **36**, 1161 (2006) [*Quantum Electron.*, **36**, 1161 (2006)].
8. Bouwmans G., Segard B., Glorieux P., Milovsky N., Khandokhin P., Shirokov E. *Izv. Vyssh. Uchebn. Zaved., Ser. Radiofiz.*, **47**, 813 (2004).
9. Ievlev I.V., Khandokhin P.A., Shirokov E.Yu. *Kvantovaya Elektron.*, **36**, 228 (2006) [*Quantum Electron.*, **36**, 228 (2006)].
10. Kravtsov N.V., Lariontsev E.G., Naumkin N.I. *Kvantovaya Elektron.*, **34**, 839 (2004) [*Quantum Electron.*, 34, 839 (2004)].
11. Molchanov V.Ya., Skrotskii G.V., *Kvantovaya Elektron.*, **1** (4), 3 (1971) [*Sov. J. Quantum Electron.*, **1** (4), 315 (1971)].
12. Nilsson A.C., Gustafson E.K., Byer R.L. *IEEE J. Quantum Electron.*, **25**, 767 (1989).
13. Novikov M.A., Tertyshnik A.D. *Izv. Vyssh. Uchebn. Zaved., Ser. Radiofiz.*, 19, 364 (1976).